Green laser annealing with metal absorber

K. Shibahara, A. Matsuno, E. Takii, K. Kurobe, and T. Eto
Research Center for Nanodevices and Systems, Hiroshima University
1-4-2, Kagamiyama, Higashihiroshima, 739-8527 Japan
Phone +81-824-24-6267, FAX: +81-824-22-7185, s-mail: shiba@sxsys.hiroshima-u.ac.jp

1. Introduction

Ultra-shallow low-resistive junction formation is a key technology for MOSFET scaling. Micro- to nanoseconds short-duration annealing is currently being developed for sub 20 nm junction formation [1-4]. We have obtained a sheet resistance of 460 Ω/sq. for the junction depth of about 20 nm using KrF excimer Laser Annealing (LA) [2]. However, high-power excimer laser has a problem concerning equipment size and maintenance. In this paper, LA with 532 nm all-solid-state green laser is described. Because of deep penetration depth in Si, about 1 μm, most part of laser energy is consumed for meaningless heating (Fig. 1). As a result, E_L (laser energy density) necessary for the dopant activation becomes lager. We introduced a light absorber that has small penetration depth to solve this problem [5]. The absorber reduced E_L necessary for dopant activation. Utilizing one-dimensional thermal diffusion analysis, part of experimental results were explained [6].

2. Sample preparation and simulation model

TiN and Mo were chosen as candidates of the absorber. Since they form silicide reacting with Si by high temperature processing, direct deposition of these materials on a Si substrate should be avoided. Sample structure is illustrated in Fig. 2. A 2 nm oxide layer was formed on a silicon substrate before depositing the absorber. The oxide was used for screen oxide and reaction barrier. Then, Sb^+ was implanted. A surface of some specimens were pre-amorphized with Ge^+ prior to the Sb^+ implantation. After the ion implantation, TiN or Mo was deposited on the screen oxide as the light absorber. The pulse width of all-solid-state green laser was 120 ns.

Thermal diffusion during LA was analyzed with a simple one-dimensional thermal diffusion model. Thermal diffusion and generated heat by the laser absorption was formulated assuming heat insulation at the surface and constant temperature at the bottom. Thermal conductivity for each material was treated as a function of temperature. Reflectivity for Si was inherent in each Si phase. The phase transition between solid-Si and liq-Si was expressed with an enthalpy-based method.

3. TiN and Mo absorber

Figure 3 shows relationships between sheet resistance and E_L for the various specimens. Sheet resistance reduction from several kΩ/sq. to about 1 κΩ/sq. is mainly explained by a-Si melting by laser heating, as discussed in our previous reports [2, 7]. By the introduction of TiN absorber, E_L necessary to make the sheet resistance be lower than 1 kΩ/sq. was decreased by about 0.3 J/cm^2, as expected. On the other hand, Mo absorber oppositely increased the E_L by 0.4 J/cm^2.

One-dimensional thermal diffusion was analyzed to explain these results. Figure 4 shows the calculated relationship between melt depth and E_L. Reduction in melting threshold E_L by TiN absorber was qualitatively explained However, increase in the E_L by Mo absorber was not. Large difference in thermal conductivity should be noted. Thermal Conductivities for Mo and TiN are 85 Wcm^{-1}K^{-1} and 8.4 Wcm^{-1}K^{-1} at about 1300^{O}C. High thermal conductivity of the absorber gives rise to not negligible thermal diffusion to outside of the irradiation area. Two-dimensional simulation that can treat lateral thermal flow is necessary to clearly discuss this problem.

Figure 5 shows variation in Sb depth profiles due to E_L increase. In the case of no absorber, in spite of large E_L difference, obtained junction depth was almost constant. On the other hand, for the specimen with the TiN absorber, E_L increase by only 0.2 J/cm^2 lead to severe junction spreading indicating melting of both a-Si and underneath c-Si layers. Therefore, process window to form shallow junction is very narrow for the TiN absorber. This difference is attributed to the absence of a negative feedback effect by reflectivity reduction due to surface melting. In the case of annealing without the absorber, surface melting decreases effective laser energy density for the latter half of laser pulse duration because of high liq-Si reflectivity. Since a metal absorber does not show such a change in reflectivity, most part of irradiated light was absorbed. Thus, over-melt to c-Si was brought about for the specimen with the TiN absorber.

4. Summary

Green laser annealing with the light absorber has been investigated. By adding a TiN absorber layer, sheet resistance lower than 1 kΩ/sq. was obtained for the lower E_L. Though this result was explained with one-dimensional thermal diffusion analysis, the Mo absorber that needed higher E_L for activation was not well explained. Lateral thermal flow should be considered to treat a high thermal conductivity film like Mo. Narrowing of process window against E_L was attributed to the absence of reflectivity reduction mechanism.

Acknowledgements

This work was partly supported by NEDO/MIRAI Project. We thank Dr. T. Kudo, Sumitomo Heavy Industries Ltd. for his cooperation concerning laser annealing.

References

[1] B. Yu et al., IEEE IEDM Tech. Digest, 1999, p. 348.
[2] K. Kurobe et al., Ext. Abst. USJ Workshop, 2003, p. 98.
[3] A. Shima et al., IEEE IEDM Tech. Digest, 2003, p. 493.
[4] T. Ito et al., Ext. Abst. of IWJT, 2002, p. 23.
[5] Takii et al., submitted to Jpn. J. Appl. Phys. Part II.
[6] A. Matsuno et al., submitted to Nucl. Instr. and Meth. B.
[7] K. Kurobe, et al., Ext. Abst. IWJT, 2002. p. 35.

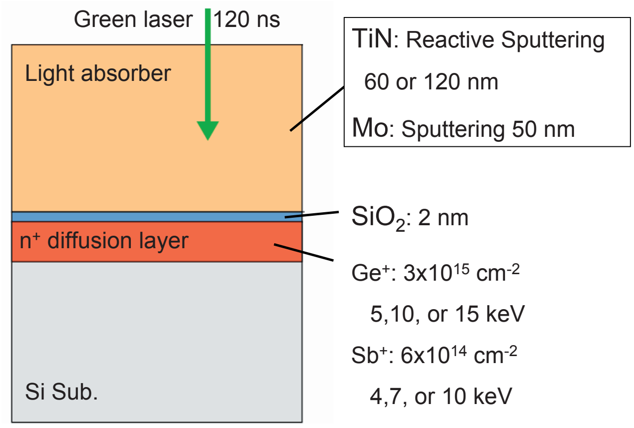

Fig. 2 Specimen structure and film thickness.

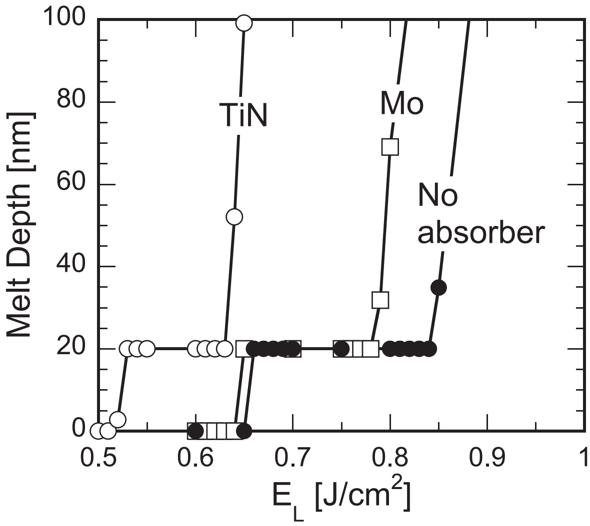

Fig. 4 Simulated melt depth against E_L to discuss effectiveness of absorber.

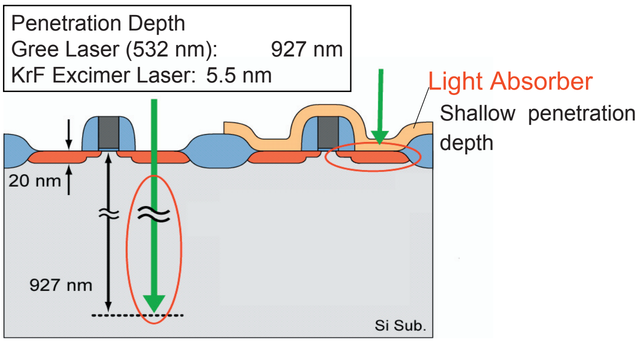

Fig. 1: Light penetration depth in Si and device dimension.

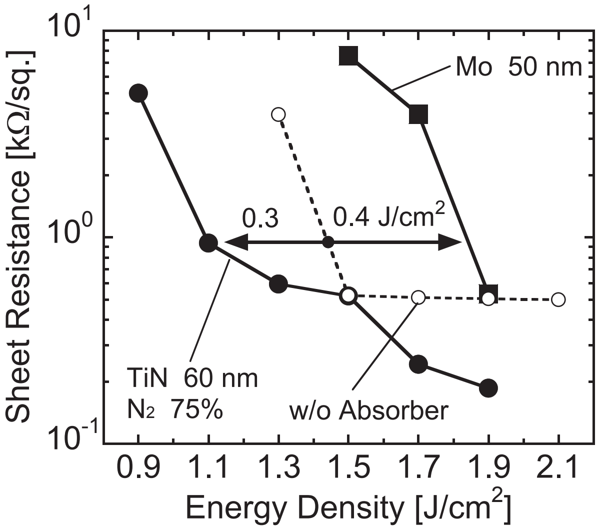

Fig. 3 Relationships between E_L and sheet resistance. The TiN absorber decreased E_L necessary for dopant activation, but Mo increased.

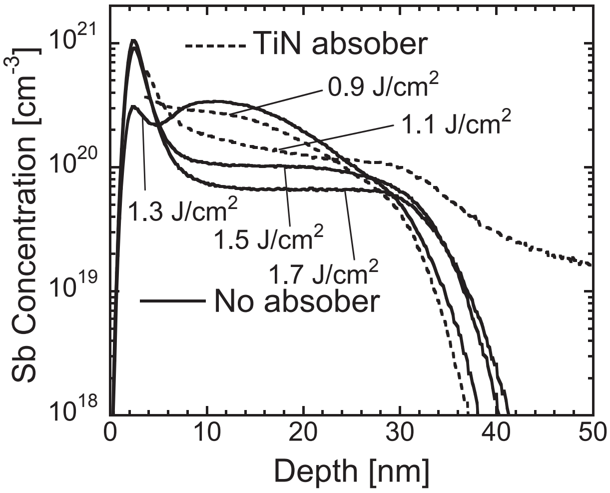

Fig. 5 Sb depth profiles for various laser energy densities to compare process window width against E_L for the no absorber case (solid line) and the TiN absorber case (dashed line).

Green Laser Annealing with Metal Absorber

K. Shibahara, A. Matsuno, E. Takii, K. Kurobe, and T. Eto

Research Center for Nanodevices and Systems,
Hiroshima University

1-4-2, Kagamiyama, Higashihiroshima, 739-8527 Japan
Phone +81-82-424-6267, FAX: +81-82-424-3499
e-mail: shiba@sxsys.hiroshima-u.ac.jp

Motivation

Shallow Junction Formation (< 20 nm)

RTA, Spike-RTA....

What is next?

Solid phase regrowth:	min to hr
FLASH lamp:	μs – ms
CW Laser Annealing (Non-Melt):	μs – ms
Pulse Laser Annealing (Melt):	ns

nanoseconds Laser Annealing is ultimate one
to obtain non-thermal equilibrium

Selection of Laser Source

Shallow Junction Formation (<20 nm) KrF Excimer Laser

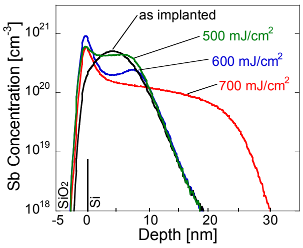

IWJT 2002 Kurobe et al.

Hiroshima Univ.

High Power Excimer Laser
Issues: Equipment size and maintenance

All-Solid-State Green Laser (λ: 532 nm)
Solutions for the issues

Penetration Depth

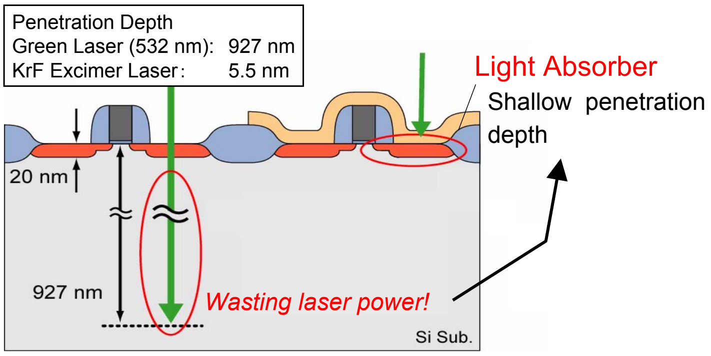

Penetration Depth

Green Laser (532 nm):	927 nm
KrF Excimer Laser:	5.5 nm

Light Absorber

Shallow penetration depth

Wasting laser power!

Requirements for Absorber

- Shallow penetration depth
- High thermal conductivity
- High thermal stability

→ Refractory metal
or
Barrier metal
+
Insulator

Candidates

- TiN
- Mo

} + SiO₂

Light Absorber *Reaction Barrier*

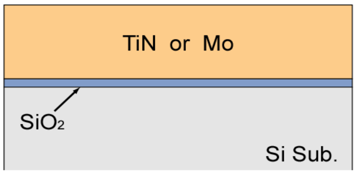

Sample Structure

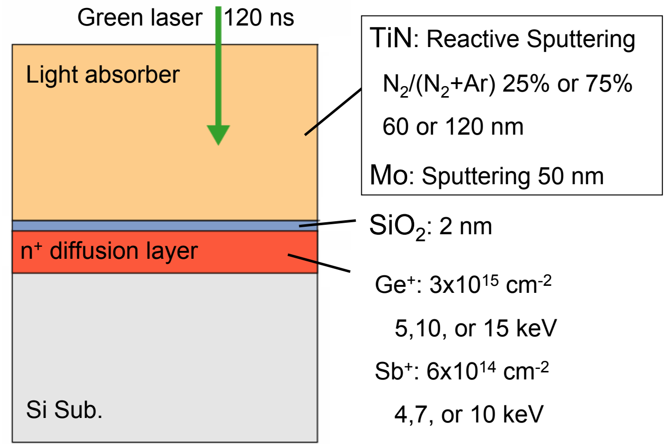

TiN: Reactive Sputtering
N$_2$/(N$_2$+Ar) 25% or 75%
60 or 120 nm

Mo: Sputtering 50 nm

SiO$_2$: 2 nm

Ge$^+$: 3x10^{15} cm^{-2}
5,10, or 15 keV
Sb$^+$: 6x10^{14} cm^{-2}
4,7, or 10 keV

Depth Profile: No absorber

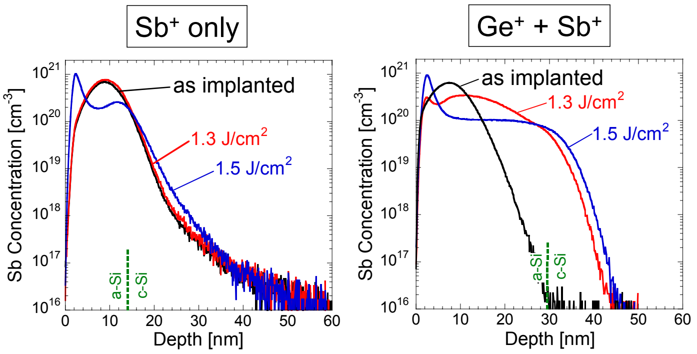

- Junction depth is controlled by amorphization depth.
- E_L(Laser energy density) for melting > 1.3 J/cm^2

Depth Profile: TiN absorber

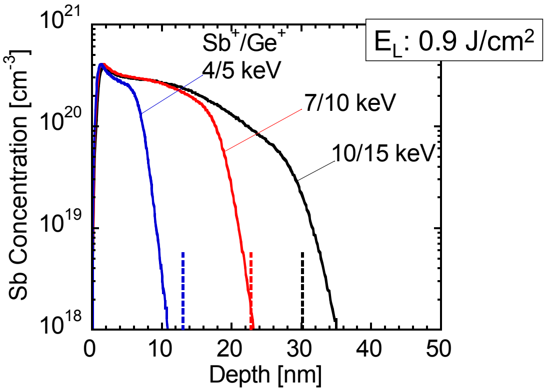

- X_j < 10 nm is obtainable with absorber
- E_L for melting ~ 0.9 J/cm^2 ← Reduced

Comparison of TiN and Mo Absorbers

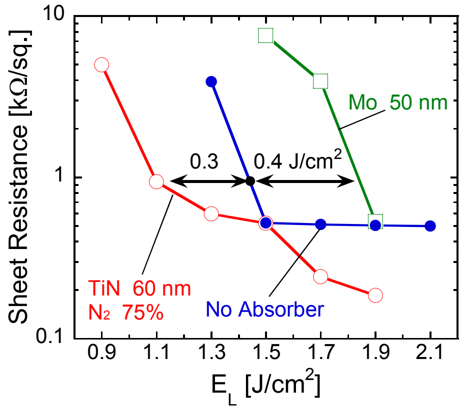

- E_L for melting: TiN decreased
  Mo increased

One-dimensional Thermal Diffusion Simulation

$$\begin{cases} c\rho\dfrac{\partial T(x,t)}{\partial t} = \dfrac{\partial}{\partial x}\left(\kappa(T)\dfrac{\partial T(x,t)}{\partial x}\right) + \alpha(1-R)I(x,t) \\ \left.\dfrac{\partial T}{\partial x}\right|_{x=0} = 0 \\ T_{x=L} = T_0, \quad T_{t=0} = T_0 \end{cases}$$

c : specific heat
ρ : density
κ : thermal conductivity
α : absorption coefficient
R : Reflectivity
I : laser power density

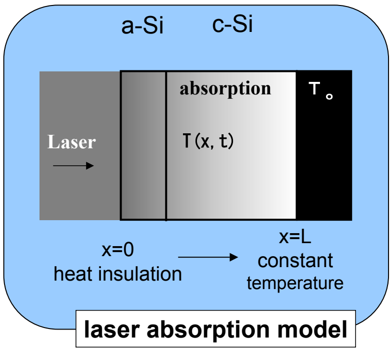

Comparison with Simulation

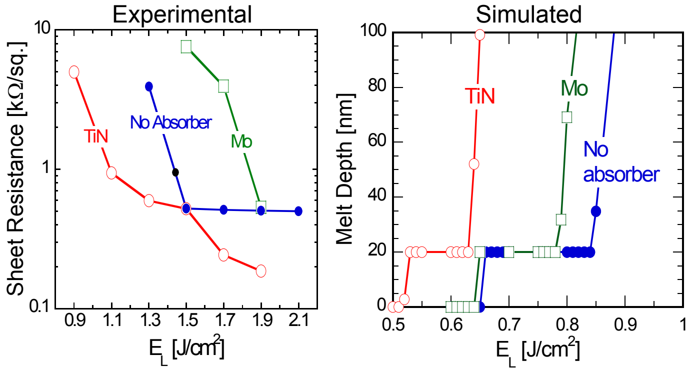

- TiN and No Absorber: Qualitatively explained by simulation
- Mo: Discrepancy

TiN and Mo

E_L for Melt : Mo > No absorber

Reflectivity (included in simulation)

Si	38%
TiN	30%
Mo	58%

- Difference in reflectivity is not enough to explain

Thermal Conductivity

Mo 113 W/m/K >> TiN 11 W/m/K @ 700°C

- Mo: Lateral thermal conduction should be considered

Process Window Width

Experimental Results

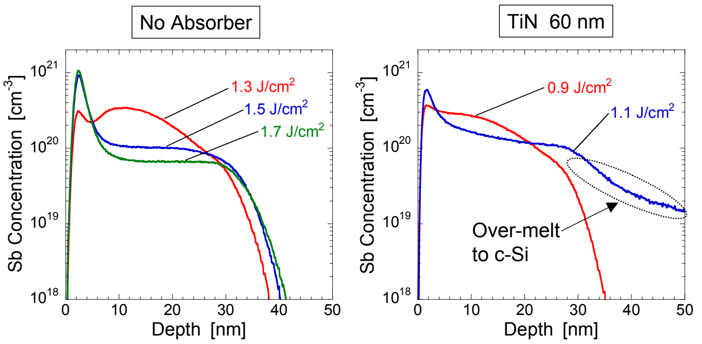

- TiN: Narrow process window against E_L variation

Influence of Reflectivity Change

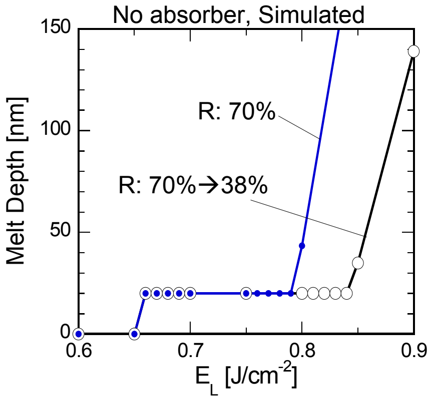

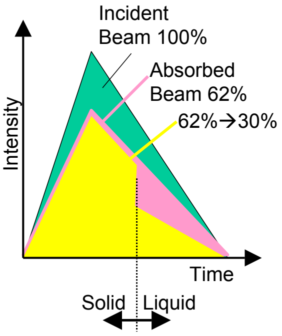

c-Si, a-Si: Semiconductive R=0.38

liquid-Si: Metallic R=0.70

Origin of Narrow Process Window

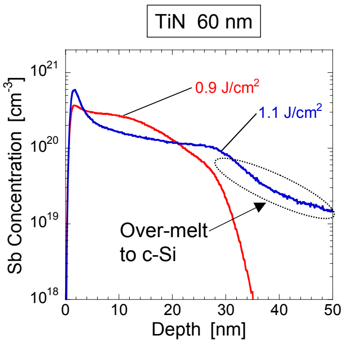

Metal absorber:

No stopping mechanism against c-Si overmelt

Conclusions

Green laser annealing with light absorber

Results

- TiN→ E_L reduction, Mo: NG

  Lateral thermal diffusion should be considered to explain this

- Over-melt, narrow process window

  Absence of feedback mechanism

Acknowledgements

Part of this work was supported by NEDO/MIRAI project.
The authors thank to Sumitomo Heavy Industry
for their cooperation.